

Electronic Supplementary Information

Precisely Regulating the Double-Boron-based Multi-Resonance Framework towards Pure-Red Emitters: High-Performance OLED with CIE Coordinates Fully Satisfying BT. 2020 Standard

Yang Zou, Jiawei He, Nengquan Li, Yuxuan Hu, Sai Luo, Xiaosong Cao, Chuluo Yang**

Shenzhen Key Laboratory of New Information Display and Storage Materials,
College of Materials Science and Engineering, Shenzhen University, Shenzhen
518060, PR China

Yang Zou e-mail: yangzou@szu.edu.cn

Chuluo Yang e-mail: clyang@szu.edu.cn

Table of contents

General information	2
Quantum Chemical Calculations.....	3
Device Fabrication and Characterization.....	3
Synthesis of the materials	4
¹H NMR , ¹³C NMR and HR-MS spectroscopies	7
Thermal and electrochemical properties	15
Theoretical simulation	15
Photophysical properties	16
Supplemental electroluminescence data	17

General information

Unless otherwise indicated, all starting materials were obtained from commercial suppliers and were used without further purification. All the reaction solvents were purified by solvent purification system prior to use.

The ¹H and ¹³C nuclear magnetic resonance (NMR) spectra were recorded in deuterated chloroform (CDCl₃) solution on Bruker NMR spectrometer with tetramethylsilane (TMS, δ 0.00) as the internal standard. High-resolution electrospray (ESI) mass spectra were performed on SCIEX TripleTOF6600 nanoLCMS. Thermogravimetric analysis (TGA) was undertaken using a PerkinElmer Instruments (Pyris1 TGA) at a heating rate of 10 °C/ min from 30 to 800 °C under a nitrogen environment. UV-vis absorption spectra were recorded on a Shimadzu UV-2700

recording spectrophotometer. Photoluminescence (PL) spectra were recorded on a Hitachi F-4600 fluorescence spectrophotometer. The lifetimes of fluorescence and delayed fluorescence were performed on PicoQuant Fluotime300. Absolute PLQYs were obtained using a Quantaaurus-QY measurement system (C9920-02, Hamamatsu Photonics). Cyclic voltammetry (CV) was carried out in nitrogen-purged dichloromethane (oxidation scan) at room temperature with a CHI voltammetric analyzer. Tetrabutylammonium hexafluorophosphate (TBAPF₆) (0.1 M) was used as the supporting electrolyte. The conventional three-electrode configuration consists of a platinum working electrode, a platinum wire auxiliary electrode, and an Ag wire pseudo reference electrode with ferrocenium/ferrocene (Fc⁺/Fc) as the internal standard.

Quantum Chemical Calculations

All of the simulation calculations were carried out with Gaussian 09 program package. The ground state geometries were optimized *via* density functional theory (DFT) calculations in vacuum using the B3LYP-D3(BJ) hybrid functional and the 6-31G(d,p) basis set. The density functional dispersion correction was conducted by Grimme's D3 version with Becke-Johnson damping function. Excited state analysis by time-dependent DFT (TD-DFT) were performed at the B3LYP-D3(BJ)/6-31G(d,p) level on the basis of optimized ground-state geometries.

Device Fabrication and Characterization

The ITO coated glass substrates with a sheet resistance of 15 Ω square⁻¹ were consecutively ultrasonicated with acetone/ethanol and dried with nitrogen gas flow, followed by 20 min ultraviolet light-ozone (UVO) treatment in a UV-ozone surface processor (PL16 series, Sen Lights Corporation). Then the sample was transferred to the deposition system. Both 8-hydroxyquinolinolato-lithium (Liq) as electron injection layer and aluminum (Al) as cathode layer were deposited by thermal evaporation at 5×10^{-5} Pa. Additionally, the organic layers were deposited at the rates

of 0.2-3 Å/s. After the organic film deposition, Liq and Al layer were deposited with rates of 0.1 and 3 Å/s, respectively. The emitting area of the device is about 0.09 cm². The current density-voltage-luminance (*J-V-L*), L-EQE curves and electroluminescence spectra were measured using a Keithley 2400 source meter and an absolute EQE measurement system (C9920-12, Hamamatsu Photonics, Japan).

Synthesis of the materials

Synthesis of 1,4-dibromo-2-(4-(*tert*-butyl)phenoxy)-3,5,6-trifluorobenzene (1O3F): To a 100 mL flask was added 1,4-dibromotetrafluorobenzene (5.00 g, 16.23 mmol), 4-(*t*-butyl)phenol (2.40 g, 16.23 mmol), Cs₂CO₃ (5.80 g, 17.85 mmol) and dry DMF (50 mL). The mixture was stirred at 60°C for 12h under argon. After cooling to room temperature, the reaction mixture was poured into water and extracted with dichloromethane. The organic layer was dried by anhydrous sodium sulfate, and the organic solvent was removed under reduced pressure. The crude product was further purified by silica gel column chromatography using DCM/PE as the eluent (*v/v* = 1:5). The product was obtained as colorless oil, and then slowly solidified as white solid in the yield of 52%. ¹H NMR (500 MHz, CDCl₃) δ 7.32 (dd, *J* = 8.5, 1.3 Hz, 2H), 6.83-6.77 (m, 2H), 1.30 (s, 9H). ¹⁹F NMR (377 MHz, CDCl₃) δ -121.37 (d, *J* = 9.3 Hz), -129.51 – -129.63 (m), -129.99, -130.02, -130.08. ¹³C NMR (126 MHz, CDCl₃) δ 154.56, 150.04 (*d*, *J* = 250 Hz, 1C), 146.37, 146.03 (*q*, *J* = 242 Hz, 9 Hz, 1C), 145.61 (*q*, *J* = 242 Hz, 9 Hz, 1C), 137.99 (*q*, *J* = 13 Hz, 5 Hz, 1C), 126.65, 114.68, 107.23 (*d*, *J* = 19.8 Hz, 1C), 99.27 (*t*, *J* = 22.5 Hz, 1C), 34.29, 31.44. HRMS: (ESI) *m/z* calcd for C₁₆H₁₄OBr₂F₃ [M+H]⁺: 438.9338; found: 438.9318.

Synthesis of M1: To a 100 mL flask was added 1O3F (1.89 g, 4.31 mmol), carbazole (4.00 g, 14.31 mmol), *t*-BuOK (1.59 g, 14.24 mmol) and dry DMF (40 mL). The mixture was stirred at 150°C for 12h under argon. After cooling to room temperature, the reaction mixture was poured into water and the resulting solid was collected by filtration. The crude product was washed thoroughly with 100 mL of hot ethanol and further purified by silica gel column chromatography using DCM/PE as

the eluent ($v/v = 1:3$). The product was obtained as a white solid in the yield of 70%. ^1H NMR (400 MHz, CDCl_3) δ 7.94 (dt, $J = 7.8, 1.0$ Hz, 2H), 7.76 (dt, $J = 7.6, 1.0$ Hz, 2H), 7.72 (dt, $J = 7.8, 1.0$ Hz, 2H), 7.43 (ddd, $J = 8.2, 7.2, 1.2$ Hz, 2H), 7.22-7.01 (m, 16H), 6.73-6.68 (m, 2H), 6.16-6.08 (m, 2H), 1.02 (s, 9H). ^{13}C NMR (125 MHz, CDCl_3) δ 154.50, 153.61, 146.42, 139.26, 139.23, 139.16, 139.15, 138.90, 135.26, 132.00, 129.60, 125.73, 125.57, 125.19, 123.64, 123.55, 123.40, 122.26, 120.57, 120.38, 120.26, 120.14, 120.09, 120.03, 119.98, 115.18, 110.53, 110.33, 110.31, 77.22, 77.01, 76.80, 33.85, 31.21. HRMS: (ESI) m/z calcd for $\text{C}_{52}\text{H}_{38}\text{ON}_3\text{Br}_2[\text{M}+\text{H}]^+$: 880.1356; found: 880.1335.

Synthesis of M2: Compound **M2** was synthesized according to the same procedure of compound **M1**, except for using 3,6-di-*tert*-butyl-9H-carbazole as the substrate. The product was obtained as a white solid in the yield of 62%. ^1H NMR (400 MHz, CDCl_3) δ 7.95 (d, $J = 1.6$ Hz, 2H), 7.58 (d, $J = 1.6$ Hz, 2H), 7.55 (d, $J = 1.6$ Hz, 2H), 7.48 (dd, $J = 8.5, 1.7$ Hz, 2H), 7.12 (d, $J = 8.5$ Hz, 2H), 7.00 (ddd, $J = 8.2, 6.2, 1.7$ Hz, 4H), 6.82 (d, $J = 8.6$ Hz, 2H), 6.76 (dd, $J = 8.7, 2.6$ Hz, 4H), 6.24 (d, $J = 8.7$ Hz, 2H), 1.46 (s, 18H), 1.35 (d, $J = 8.9$ Hz, 36H), 1.05 (s, 9H). ^{13}C NMR (125 MHz, CDCl_3) δ 153.79, 153.36, 146.03, 143.10, 143.05, 142.94, 142.77, 138.54, 137.55, 137.30, 137.26, 137.17, 134.95, 131.75, 129.12, 125.43, 123.78, 123.75, 123.56, 123.49, 123.37, 122.56, 122.46, 121.87, 116.07, 115.53, 115.46, 115.42, 115.13, 110.16, 110.09, 109.88, 109.77, 34.73, 34.53, 34.50, 34.48, 33.90, 32.06, 31.92, 31.31. HRMS: (ESI) m/z calcd for $\text{C}_{76}\text{H}_{86}\text{ON}_3\text{Br}_2 [\text{M}+\text{H}]^+$: 1216.5112; found: 1216.5089.

Synthesis of RBNO1: To a flame-dried 120 mL pressure tube was added **M1** (3.00 g, 2.47 mmol) and ultra-dry mesitylene (30 mL). Then under 0°C and argon atmosphere, *n*-BuLi (in hexane, 2.96 mL, 7.41 mmol) was added dropwise. The reaction mixture allowed to 50°C and stirred for 2h under argon. After cooling to room temperature, the hexane was removed by vacuum pump. After cooling to -40°C , BBr_3 (1.00 mL, 10.37 mmol) was added to the reaction mixture in one portion and stirred for 10 minutes. The reaction mixture was allowed to 0°C , and DIPEA (1.81

mL, 10.37 mmol) was added dropwise under ice-water bath. The reaction mixture was heated to 165°C for 12h. After cooling to room temperature, the reaction was quenched by adding 10 mL of ethanol. The resulting mixture was poured into water and extracted with DCM three times, and the organic layer was dried with anhydrous Na₂SO₄. After removing the organic solvent under reduced pressure, the residue was purified by silica gel column chromatography using DCM/PE as the eluent (v/v = 1:3). The crude brown powder was further purified by recrystallization from DCM/methanol to give the product as a violet powder in the yield of 26%. ¹H NMR (600 MHz, toluene-*d*₈) δ 9.31-9.21 (m, 2H), 9.00 (dd, *J* = 7.4, 3.3 Hz, 1H), 8.94 (d, *J* = 7.2 Hz, 1H), 8.26-8.17 (m, 3H), 8.11-8.04 (m, 1H), 7.93-7.86 (m, 1H), 7.73-7.58 (m, 6H), 7.51 (d, *J* = 8.6 Hz, 1H), 7.37 (ddd, *J* = 6.5, 4.6, 1.7 Hz, 2H), 6.80-6.74 (m, 2H), 6.60 (d, *J* = 8.4 Hz, 1H), 6.50 (tdd, *J* = 10.2, 6.9, 5.6 Hz, 3H), 1.49 (s, 9H). ¹³C NMR (150 MHz, toluene-*d*₈) δ 156.95, 145.59, 143.24, 142.69, 142.58, 141.31, 140.60, 139.65, 139.15, 133.16, 132.86, 132.69, 131.84, 130.92, 126.59, 126.01, 125.58, 125.48, 125.22, 125.07, 124.07, 124.05, 123.28, 122.51, 122.40, 122.34, 122.03, 121.49, 121.42, 121.24, 120.89, 120.27, 120.03, 120.01, 118.18, 117.39, 111.65, 111.51, 34.41, 31.35. HRMS: (ESI) *m/z* calcd for C₅₂H₃₃ON₃B₂ [M]⁺: 737.2804; found: 737.2825.

Synthesis of RBNO2: Compound **ZYBNO2** was synthesized according to the same procedure of compound **ZYBNO1**, except for using **M1** as the substrate. The product was obtained as a dark-violet in the yield of 28%. ¹H NMR (600 MHz, toluene-*d*₈) δ 9.51 (d, *J* = 1.8 Hz, 1H), 9.48 (d, *J* = 1.8 Hz, 1H), 9.43 (d, *J* = 2.3 Hz, 1H), 9.40 (d, *J* = 1.8 Hz, 1H), 8.73 (d, *J* = 1.8 Hz, 1H), 8.70 (d, *J* = 1.7 Hz, 1H), 8.69 (d, *J* = 1.7 Hz, 1H), 8.47 (d, *J* = 2.0 Hz, 1H), 8.14 (dd, *J* = 5.4, 1.9 Hz, 2H), 7.98 (d, *J* = 8.8 Hz, 1H), 7.67-7.60 (m, 2H), 7.50 (dd, *J* = 8.8, 2.0 Hz, 1H), 6.69 (d, *J* = 8.7 Hz, 1H), 6.65-6.58 (m, 2H), 6.57 (dd, *J* = 8.7, 1.9 Hz, 1H), 1.72 (s, 9H), 1.72 (s, 9H), 1.68 (s, 9H), 1.54 (s, 9H), 1.53 (s, 9H), 1.16 (s, 18H). ¹³C NMR (150 MHz, toluene-*d*₈) δ 157.48, 145.66, 145.27, 145.15, 145.01, 144.40, 144.33, 142.76, 142.16, 142.11, 141.73, 139.85, 139.12, 138.62, 132.08, 131.32, 130.11, 130.06, 129.92, 127.14, 125.88, 125.70, 125.59, 124.16, 123.88, 123.67, 123.62, 122.27, 122.13, 121.54,

121.49, 118.58, 117.57, 116.78, 115.99, 115.93, 112.35, 112.27, 35.46, 35.43, 35.42, 34.93, 34.82, 34.56, 34.53, 32.43, 32.40, 32.36, 32.07, 31.73, 31.67. HRMS: (ESI) m/z calcd for $C_{76}H_{82}ON_3B_2$ $[M+H]^+$: 1074.6639; found: 1074.6636.

1H NMR, ^{13}C NMR and HR-MS spectroscopies

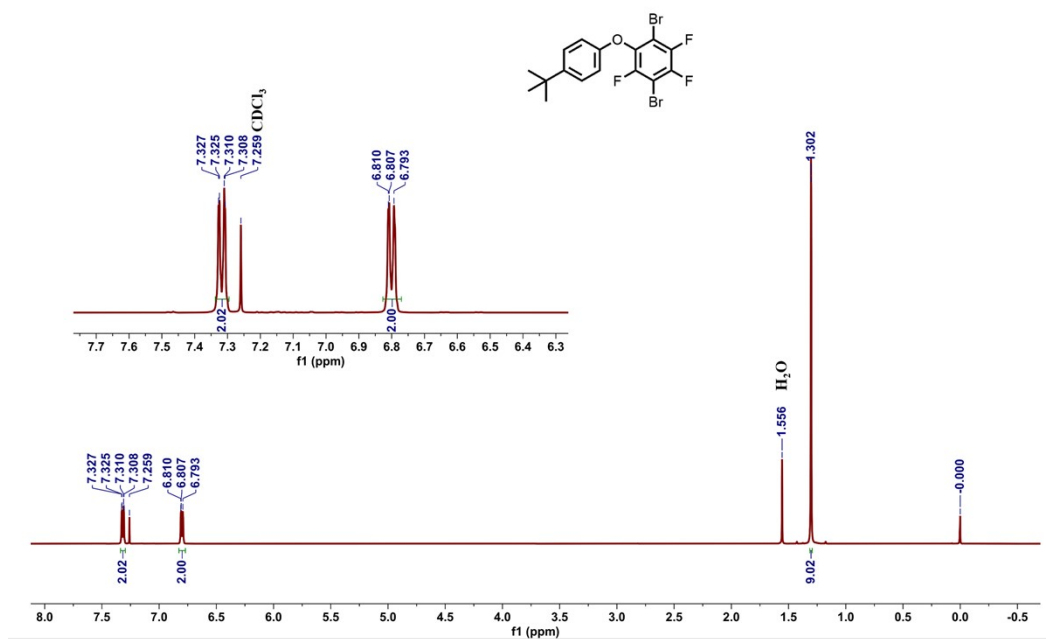


Fig. S1 1H NMR spectrum of 1O3F.

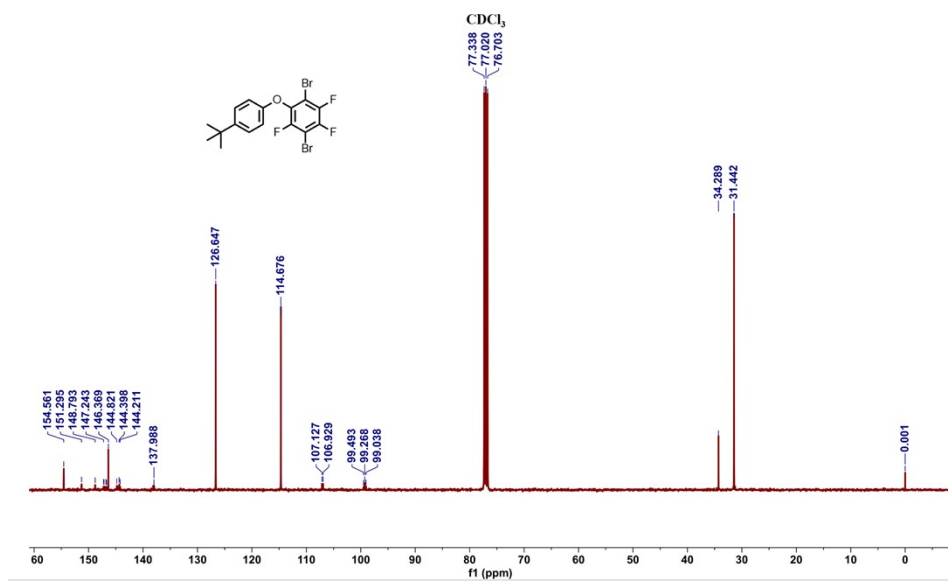


Fig. S2 ^{13}C NMR spectrum of 1O3F in $CDCl_3$.

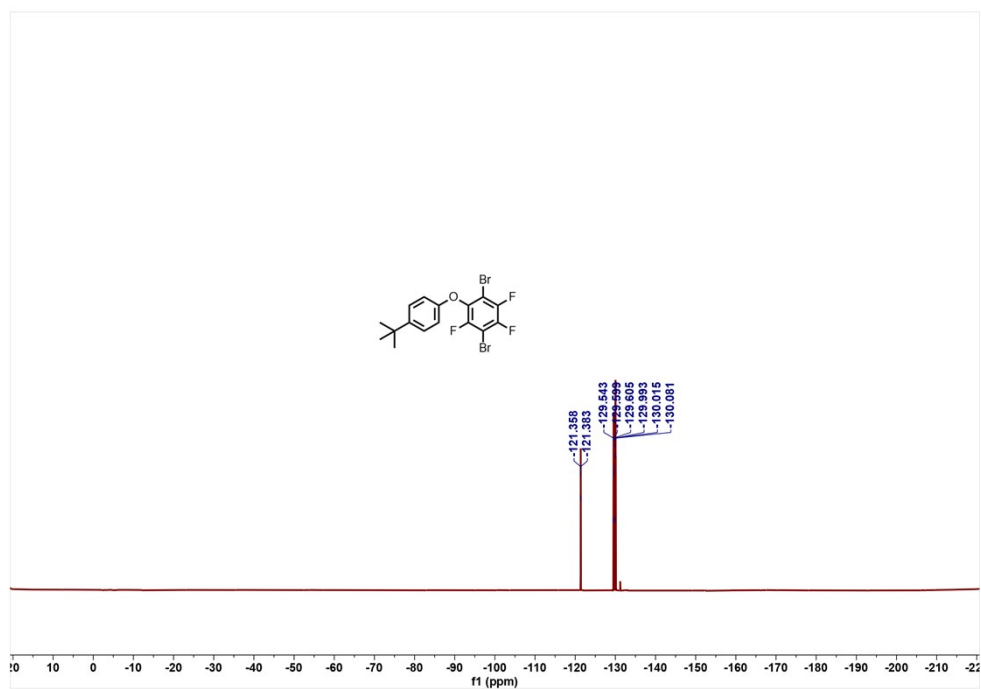


Fig. S3 ^{19}F NMR spectrum of **103F** in CDCl_3 .

103F_20230310175914 #19-41 RT: 0.20-0.42 AV: 12 NL: 1.02E6
 T: FTMS + p ESI Full ms [100.0000-800.0000]

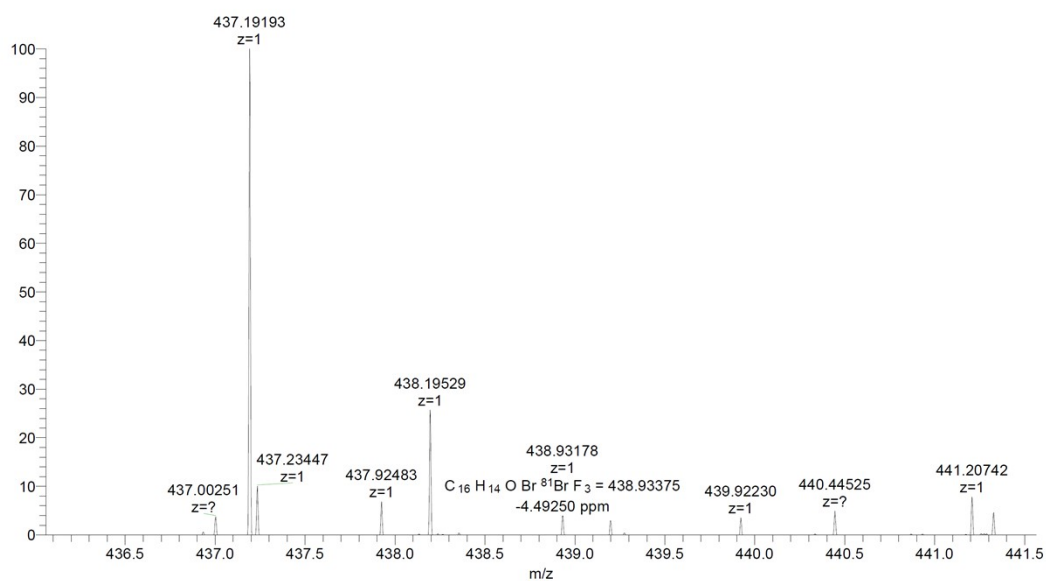


Fig. S4 HR-MS spectrum of **103F**.

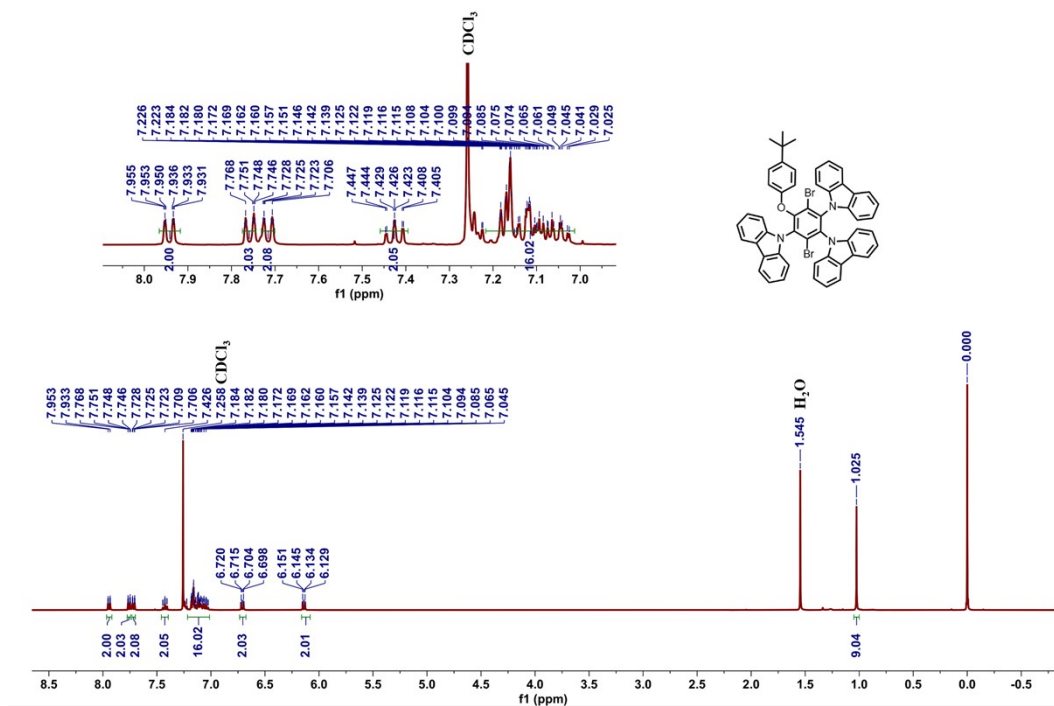


Fig. S5 ¹H NMR spectrum of M1 in CDCl₃.

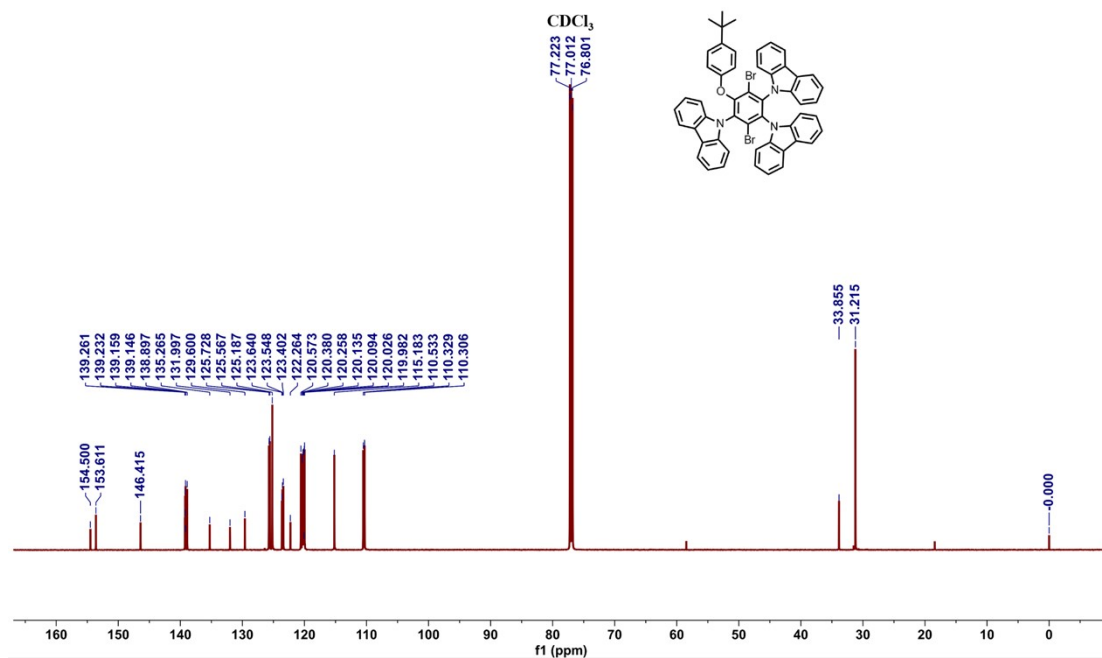


Fig. S6 ¹³C NMR spectrum of M1 in CDCl₃.

[M+H]⁺

3ClO_20230310172650 #11 RT: 0.13 AV: 1 NL: 4.02E5
T: FTMS + p ESI Full ms [500.0000-1500.0000]

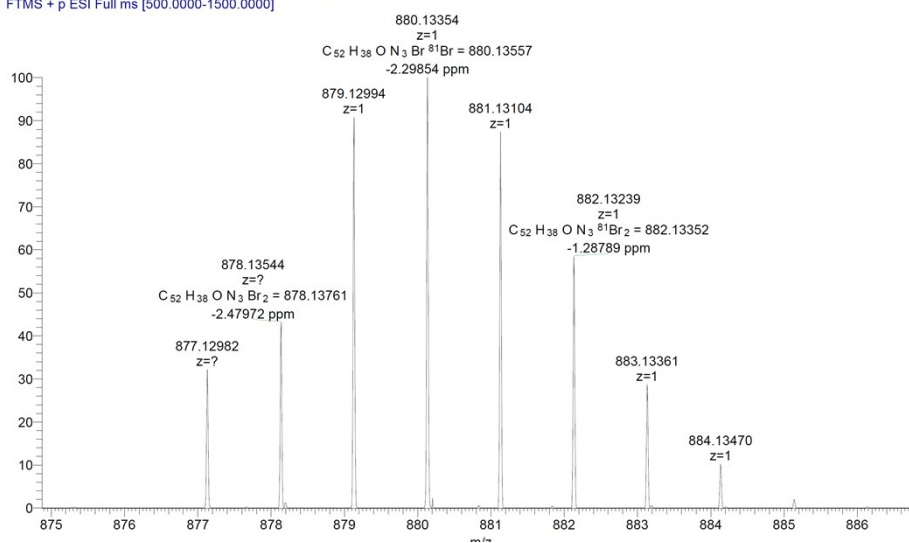


Fig. S7 HR-MS spectrum of M1.

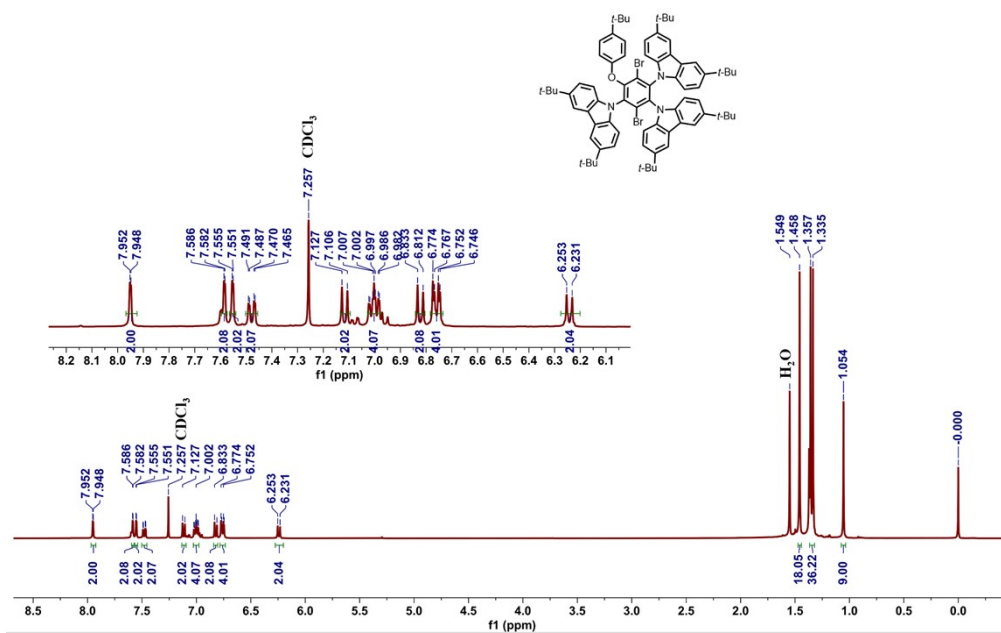


Fig. S8 ¹H NMR spectrum of M2 in CDCl₃.

[M]⁺

CZBNO_20230310172949 #31 RT: 0.38 AV: 1 NL: 9.65E5
T: FTMS + p ESI Full ms [500.0000-1500.0000]

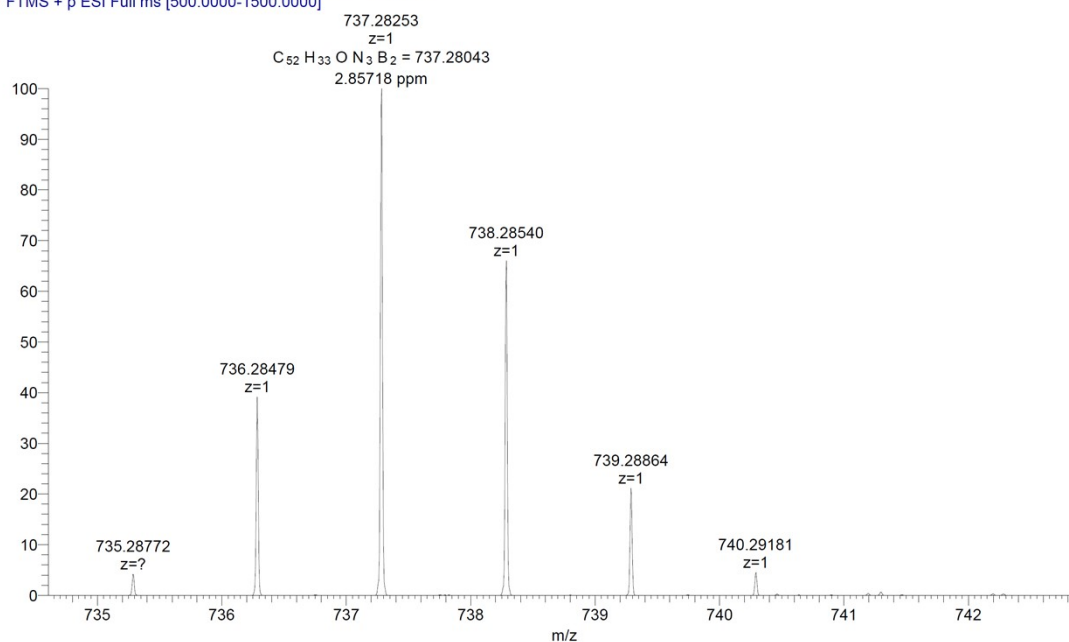


Fig. S13 HR-MS spectrum of RBNO1.

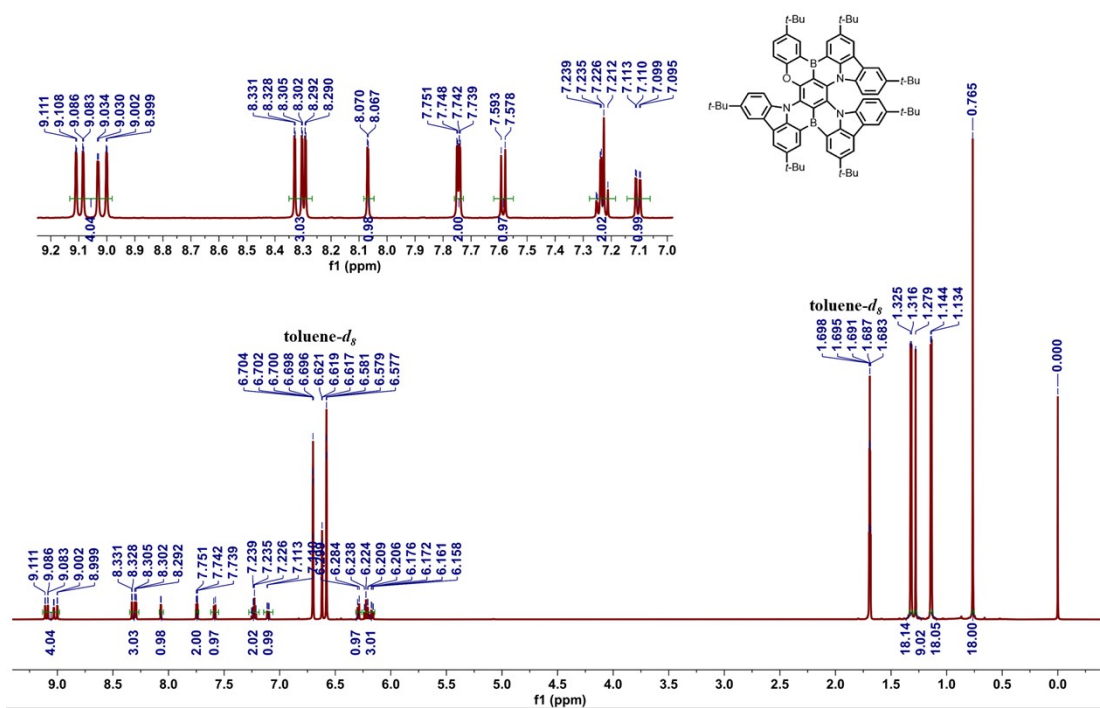


Fig. S14 ¹H NMR spectrum of RBNO2 in toluene-*d*₈.

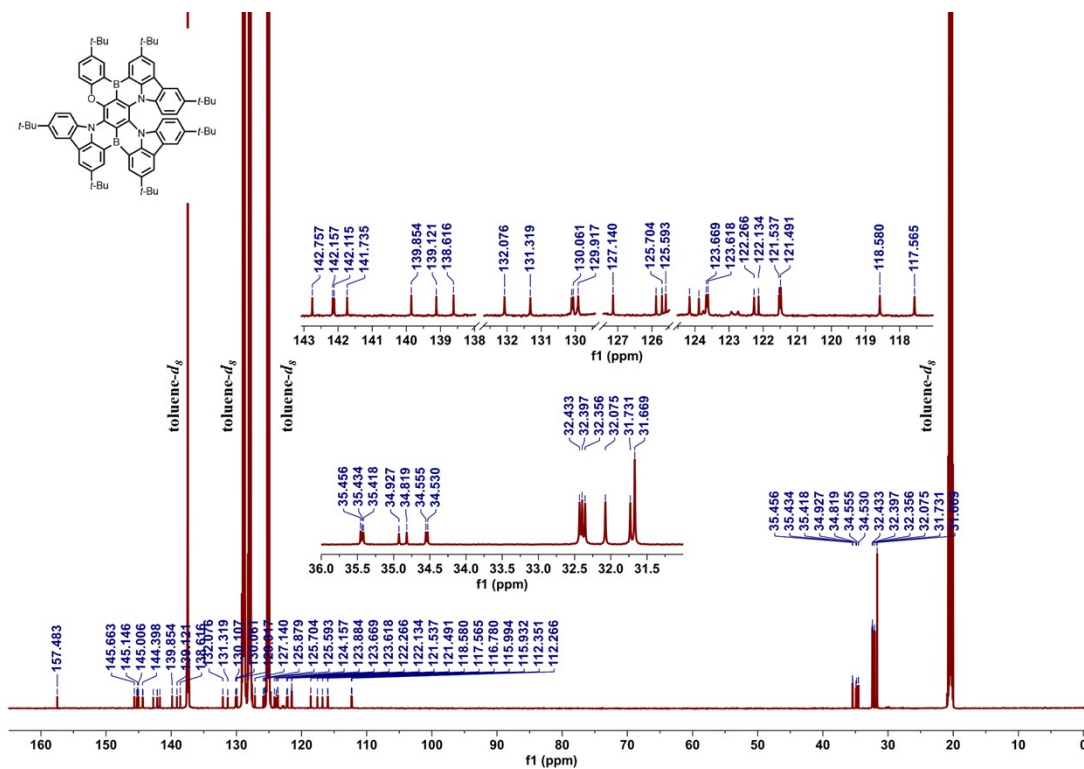


Fig. S15 ^{13}C NMR spectrum of RBNO2 in toluene- d_8 .

$[\text{M}+\text{H}]^+$

tCzBNO_20230310173220 #17 RT: 0.20 AV: 1 NL: 3.50E6
T: FTMS + p ESI Full ms [500.0000-1500.0000]

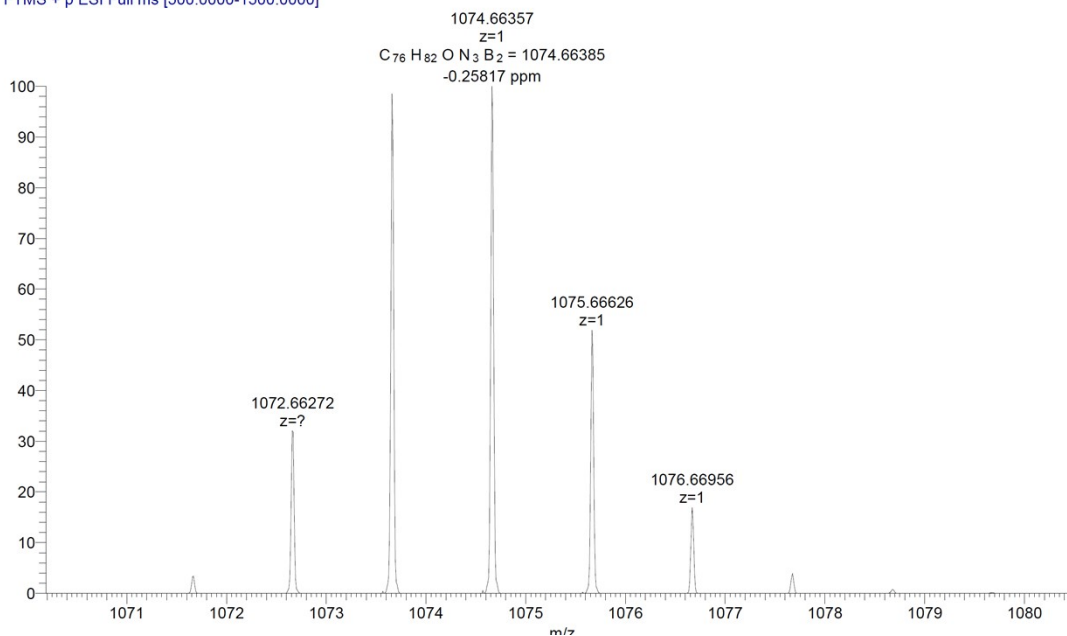


Fig. S16 HR-MS spectrum of RBNO2.

Thermal and electrochemical properties

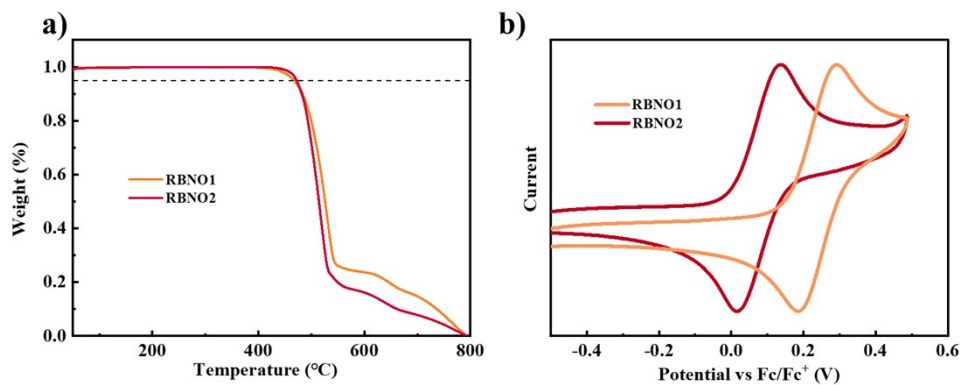


Fig. S17 a) TGA curves and b) CV curves of **RBNO1** and **RBNO2**.

Theoretical simulation

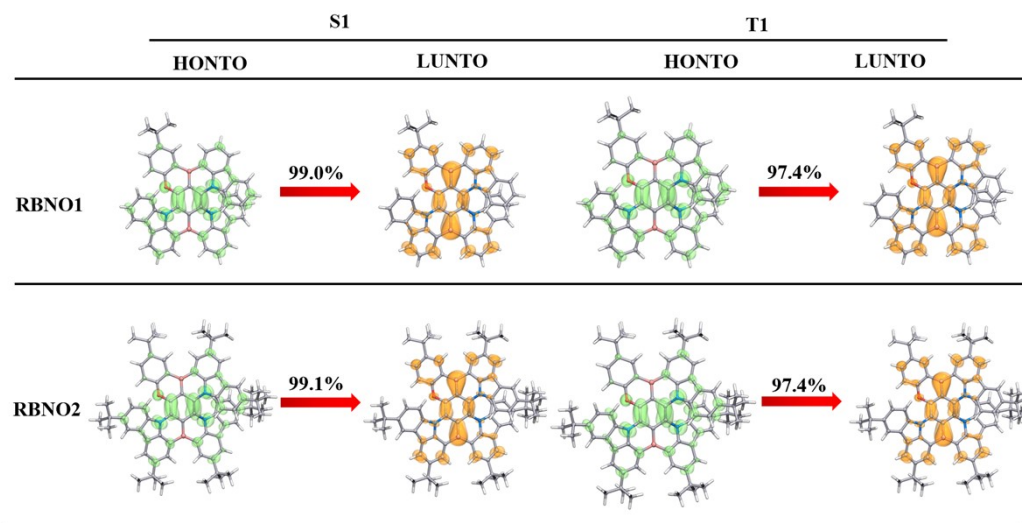


Fig. S18 The hole and electron natural transition orbitals (NTOs), eigenvalues of the corresponding NTO pairs of **RBNO1** and **RBNO2**. All results were simulated based on the optimized S1 and T1 state geometries.

Photophysical properties

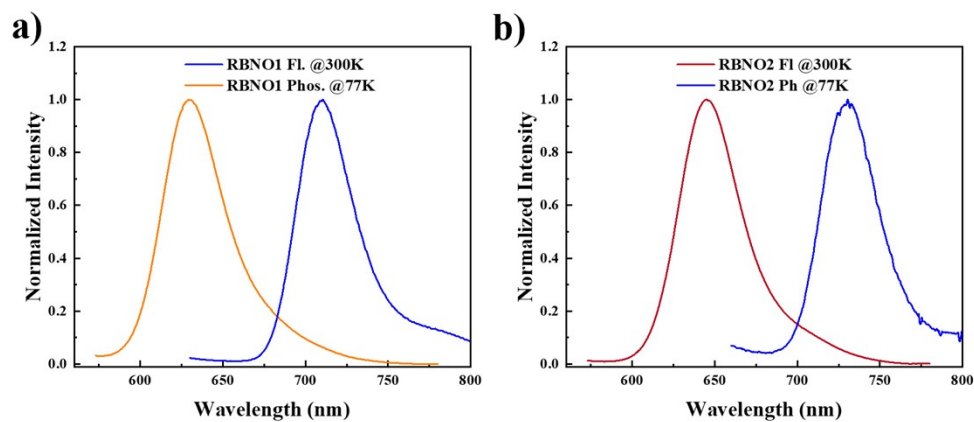


Fig. S19 Fluorescence and phosphorescent spectra of a) **RBNO1** and b) **RBNO2** in toluene solution.

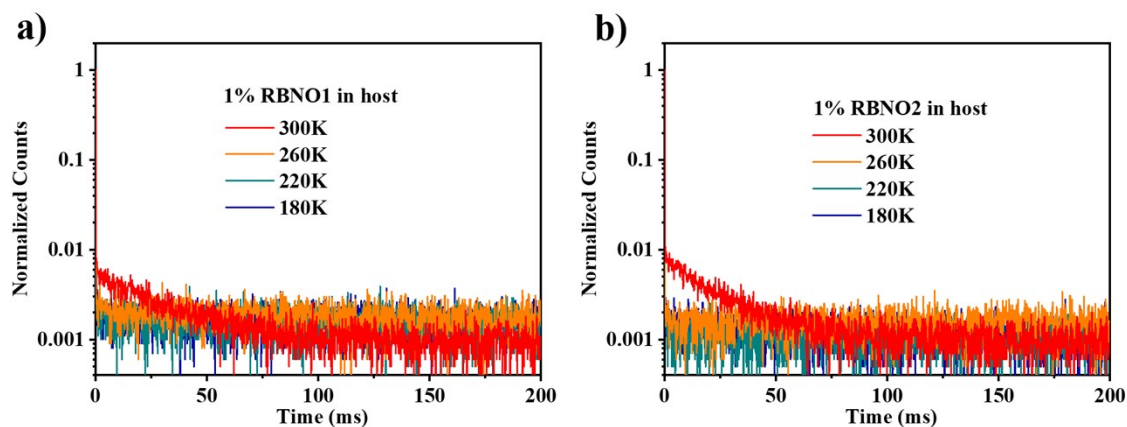


Fig. S20. Temperature-dependent transient PL decay curves of a) **RBNO1** and b)

RBNO2.

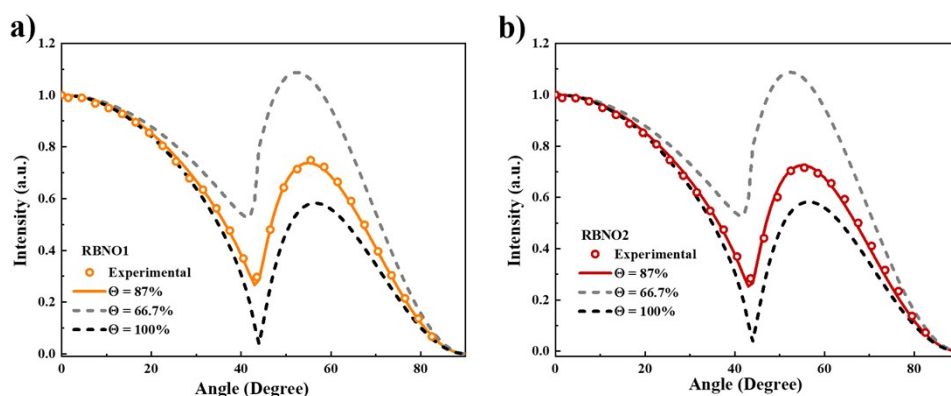


Fig. S21 The characterizations of horizontal dipole orientation by angle-dependent p -polarized PL spectra. Measured horizontal transition dipole moment ratios of a) **RBNO1** and b) **RBNO2** 1wt.% doped in DMIC-TRZ host.

Supplemental electroluminescence data

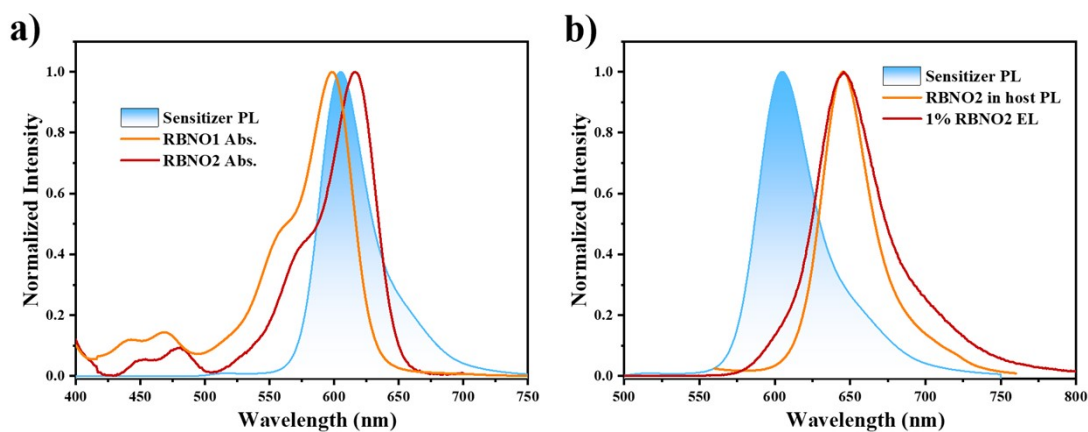


Fig. S22 a) Fluorescence spectra of sensitizer together with the absorption spectra of **RBNO1** and **RBNO2**; b) fluorescence spectra of sensitizer together with the PL spectrum and EL spectrum of **RBNO2**.

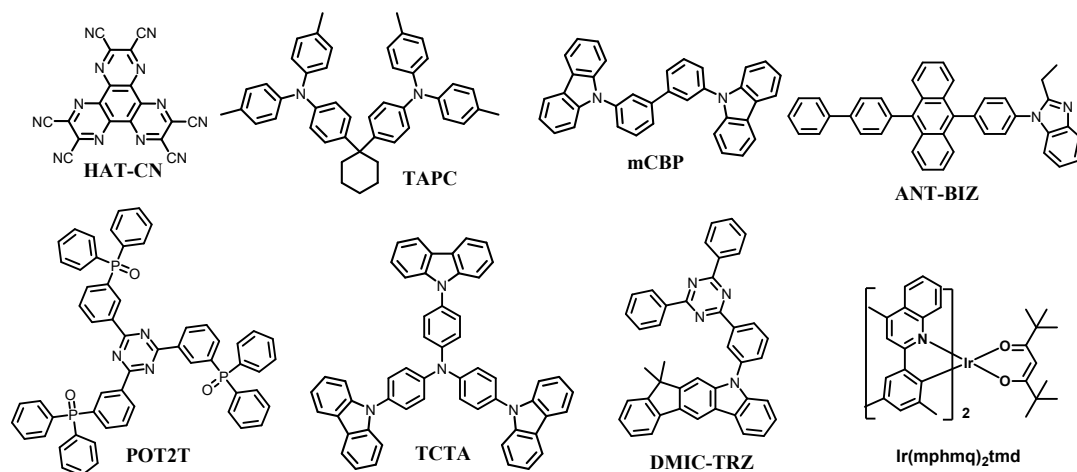


Fig. S23 Chemical structures of the materials used in the EL devices.

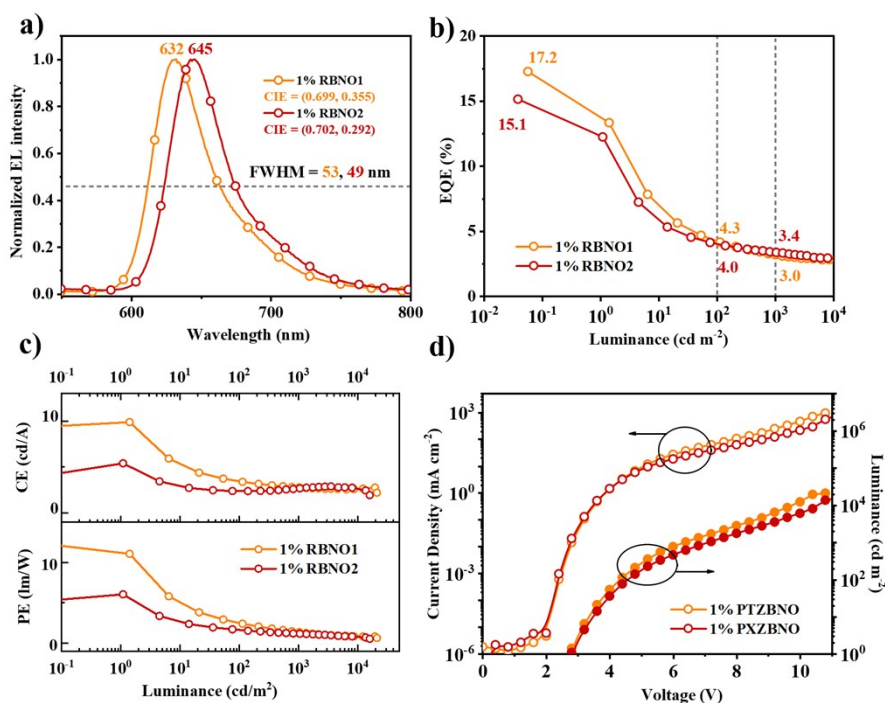


Fig. S24 a) EL spectra; b) EQE versus luminance curves; c) current efficiency and power efficiency versus luminescence curves; d) *J-V-L* curves of the non-sensitized devices

Table S1 Summary of the non-sensitized EL device data

Emitter	V _{on} (V)	L _{max} (cd/m ²)	λ _{EL} (nm)	FWHM (nm)	EQE _{max/100/1000} (%)	PE _{max} (lm/W)	CE _{max} (cd/A)
RBNO1	2.7	21100	632	53	17.2/4.3/3.0	12.3	9.4
RBNO2	2.7	16000	645	49	15.1/4.0/3.4	6.1	5.4

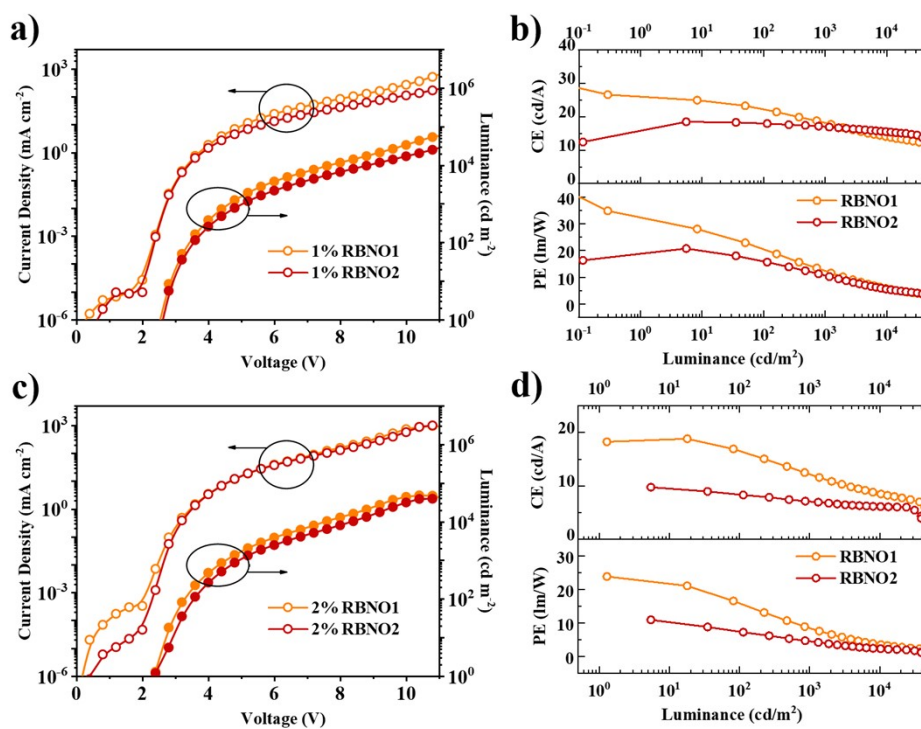


Fig. S25 *J-V-L* curves of the a) 1% doped devices c) 2% doped devices; current efficiency and power efficiency versus luminescence curves of b) 1% doped devices d) 2% doped devices.

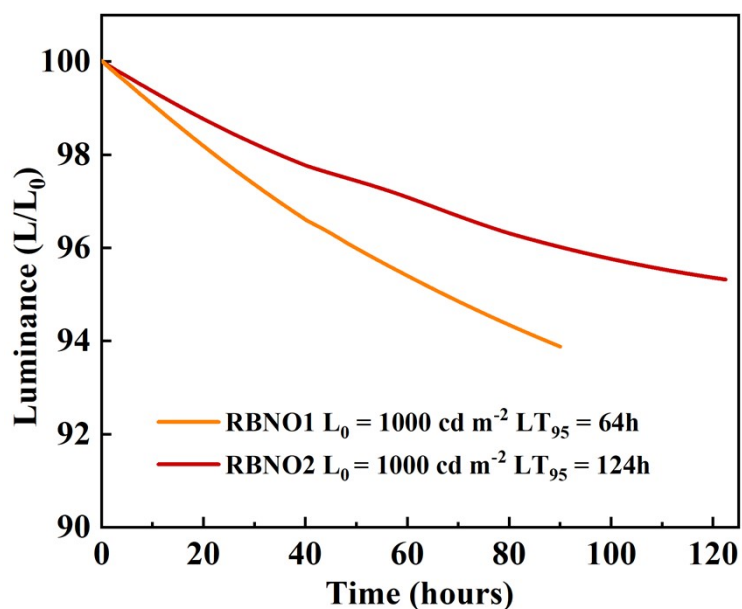


Fig. S26 Luminance decay of the OLEDs measured at the brightness of 1000 cd cm⁻².

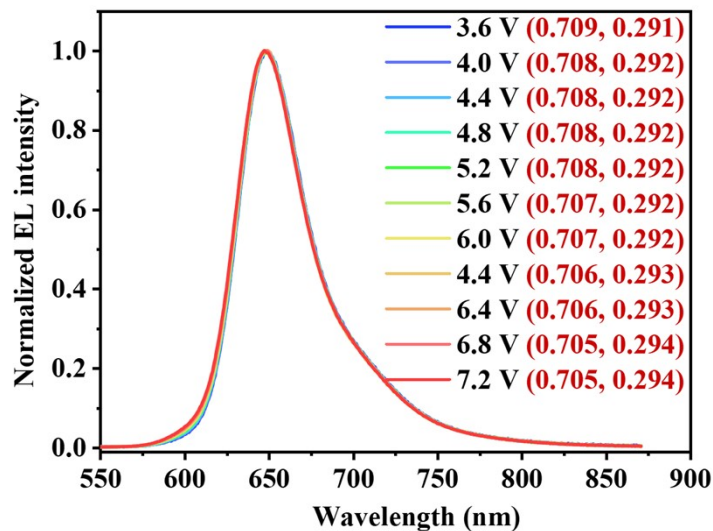


Fig. S27 EL spectra and CIE of 2% RBNO2-based device at varies driving voltages.

Table S2. The device performance of several representative red OLEDs with CIE_x over 0.66.

Emitter	λ_{em} [nm]	EQE _{max} [%]	CIE (x, y)	Reference
1% RBNO1	632	33.1	0.689, 0.311	This Work
2% RBNO1	634	27.6	0.693, 0.306	This Work
1% RBNO2	645	34.7	0.701, 0.301	This Work
2% RBNO2	648	26.6	0.708, 0.292	This Work
TPA-PZCN	648	28.1	0.66, 0.34	<i>Adv. Mater.</i> 2019 , <i>31</i> , 1902368.
PT-TPA	648	28.8	0.66, 0.34	<i>Mater. Horiz.</i> 2021 , <i>8</i> , 1297.
Ir(4tfmpq)2mND	628	30.1	0.67, 0.33	<i>ACS Appl. Mater. Interfaces</i> 2019 , <i>11</i> , 20192.
Ir(4tfmpq)2mmND	628	31.5	0.67, 0.33	<i>ACS Appl. Mater. Interfaces</i> 2019 , <i>11</i> , 20192.
Ir(4tfmpq)2mpND	620	27.7	0.66, 0.34	<i>ACS Appl. Mater. Interfaces</i> 2019 , <i>11</i> , 20192.
1F-Ir	622	26.8	0.66, 0.33	<i>Chem. Eur. J.</i> 2020 , <i>26</i> , 4410.
Ir(A2)(L2)	613	24.3	0.66, 0.34	<i>Inorg. Chem.</i> 2019 , <i>58</i> , 10944.
PPZ-BN	613	26.9	0.66, 0.34	<i>Angew. Chem. Int. Ed.</i> 2023 , <i>62</i> , e202300934.
BNNO	644	34.4	0.708, 0.292	<i>Adv. Mater.</i> 2023 , e2301018.
BN-R	618	20.1	0.663, 0.337	<i>Angew. Chem. Int. Ed.</i> 2023 , <i>62</i> , e202216473.
BNO1	625	36.1	0.66, 0.34	<i>Adv. Mater.</i> 2022 , <i>34</i> , e2201442.
BBCz-R	616	22	0.67, 0.33	<i>J. Am. Chem. Soc.</i> 2020 , <i>142</i> , 19468.
TPA-PZCN	648	28.1	0.66, 0.34	<i>Adv. Mater.</i> 2019 , <i>31</i> , 1902368.
PT-TPA	648	28.8	0.66, 0.34	<i>Mater. Horiz.</i> 2021 , <i>8</i> , 1297.
Ir(4tfmpq)2mND	628	30.1	0.67, 0.33	<i>ACS Appl. Mater. Interfaces</i> 2019 , <i>11</i> ,

20192.

BBCz-R

616

22.0

0.67, 0.33

J. Am. Chem. Soc. **2020**, *142*, 19468.
